Available online at www.sciencedirect.com
SCIENCE DIRECT®
Journal of Molecular Catalysis A: Chemical 230 (2005) 23–28
JOURNAL OF MOLECULAR CATALYSIS A: CHEMICAL
www.elsevier.com/locate/molcata

Study by in situ FTIR of the SCR of NO by propene on Cu^{2+} ion-exchanged Ti-PILC

J.L. Valverde[b], A. de Lucas[b], F. Dorado[b], A. Romero[a], P.B. García[b,*]

[a] *Facultad de Ciencias Químicas/Escuela Técnica Agrícola,Universidad Castilla-La Mancha, Campus Universitario s/n, 13071 Ciudad Real, Spain*
[b] *Departamento de Ingeniería Química, Universidad Castilla-La Mancha, Campus Universitario s/n, 13071 Ciudad Real, Spain*

Received 18 October 2004; accepted 2 December 2004

Abstract

Adsorption on Cu ion-exchanged titanium pillared clay (Cu-Ti-PILC) was investigated by in situ infrared spectroscopy to provide insight into the reaction intermediates present in the selective catalytic reduction (SCR) of NO by propene in the presence of oxygen. The NO/O_2 adsorption produced different nitrate species due to the presence of terminal and bridged Cu^{2+}–OH groups. These nitrates evolved into N_2 and N_2O in small amounts once the NO catalytic cycle was finished. It can be concluded that the Cu^{2+}–OH groups reacted with the nitro group, thus forming nitrates. C_3H_6 adsorption was higher and stronger than NO adsorption on the active sites of the catalyst. C_3H_6 reacted in the active site producing hydrocarbon intermediates (an organic nitro compound and acetate), which were responsible for the NO reduction.

Keywords: Cu; Infrared spectroscopy; NO; Pillared clays; Reaction intermediates; Selective catalytic reduction; Ti-PILC

1. Introduction

Much research related to the selective catalytic reduction of NO_x by hydrocarbons was undertaken and reported in the literature due to its potential for the effective control of NO emissions in oxidative environment [1–12]. This reaction has been described as a method to remove NO_x from natural-gas-fuelled engines, such as lean-burn gas engines in cogeneration systems [13] and lean-burn gasoline and diesel engines where the noble-metal three-way catalysts are not effective in the presence of excess oxygen [14]. Hydrocarbons would be the preferred reducing agents over NH_3 because of the practical problems associated with the ammonia use: handling and leakage through the reactor.

In 1986, Iwamoto et al. [15] reported the activity of Cu–ZSM-5 for the catalytic decomposition of NO_x. Following this finding, many catalysts such as V_2O_5-WO_3 (or MoO_3)/TiO_2, other transitions metal oxides (e.g. Fe, Cr, Co, Ni, Cu, Nb, etc.) and doped catalysts, as well as zeolite-type catalysts have been found active in this reaction.

Earlier studies were mainly focused on the developing catalysts with ZSM-5 as the porous support [16–20]. Shimizu et al. [19,20] recently reported that Cu-aluminate catalysts, containing highly dispersed Cu^{2+} ions in the aluminate phase, showed high de-NO_x activity comparable to the Cu–ZSM-5 and higher hydrothermal stability. On the other hand, Cu ion-exchanged Ti-PILCs demonstrated the best performance when using ethylene and propylene as reductants [14]. Thus, the catalytic performance of a Cu ion-exchanged Ti-PILC catalyst was found to be higher than that of Cu–ZSM-5 [21].

Recently, we have reported several studies based on the use of Ti-PILC-based catalysts for the selective catalytic reduction of NO_x using propene as the reducing agent [22–25]. It was demonstrated that Ti-PILCs ion-exchanged with Cu were the most effective catalysts for selective catalytic reduction (SCR) of NO_x, as compared to those ion-exchanged with Ni and Fe. Likewise, it was observed that the presence of 10% water in the feed inhibited the activity of the catalysts [21–23].

* Corresponding author. Tel.: +34 926 295300; fax: +34 926 295318.
E-mail address: PradoBelen.Garcia@uclm.es (P.B. García).

1381-1169/$ – see front matter © 2004 Elsevier B.V. All rights reserved.
doi:10.1016/j.molcata.2004.12.009

TPR measurements showed the presence of Cu^{2+} ions and CuO aggregates over this catalyst [22].

Many studies have also been reported about reactivity of the adsorbates and their dynamic behaviour [26–33], which is thought to be the basis for the development of a comprehensive mechanism for the SCR of NO_x with hydrocarbons.

The reaction mechanism is still the objective of many studies [30,34]. It is often claimed that the initial step for the selective reduction of NO is the formation of NO_2 through the oxidation of NO, nitrogen dioxide then reacts with the hydrocarbon to yield nitrogen-containing organic compounds, and a further reaction of this compound finally leads to the formation of nitrogen [31,34]. Sirilumpen et al. [28] proposed a reaction pathway for NO decomposition on Cu^{2+}-exchanged Al–PILC, based on in situ IR results and product analysis. The intermediates were assigned to be nitro and nitrous oxide and nitrates. In this mechanism, N_2 can be generated from nitrates or nitrous oxide decomposition.

The aim of this paper is to identify and study the stability of the species formed during NO/O_2 and $NO/O_2/C_3H_6$ adsorption on Cu-Ti-PILC by applying in situ Fourier transformed infrared (FTIR) spectroscopy.

2. Experimental

2.1. Synthesis of Ti-PILCs

The starting clay was a purified grade bentonite (Fisher Company), with a particle size <2 μm and a cation exchange capacity of 97 meq g^{-1} dry clay. Ti-PILCs were prepared as follows [22–24]. A pillaring solution was formed dissolving titanium metoxide in 5 M HCl until obtaining a molar relation HCl/metoxide of 2.5. This mixture was stirred at room temperature for 3 h. The pillaring solution was then dropped to an aqueous clay suspension until obtaining 15 mmole Ti/g clay. The mixture was kept under vigorous stirring for 12 h at room temperature. Finally, the product was washed, dried and calcined for 2 h at 400 °C. The Cu ion-exchanged sample was obtained by adding 1 g of a sample into 200 ml of 0.05 M Cu acetate solution, under stirring it for 15 h at room temperature. The ion-exchanged product was collected by centrifugation and washed several times with deionized water. The resulting catalyst was calcined for 2 h at 400 °C. The sample was denoted as Cu-Ti-PILC.

2.2. Catalyst characterization

In order to quantify the total amount of metals incorporated into the catalyst, atomic absorption (AA) measurements, with an error of ±1%, were made by using a SPECTRAA 220FS analyzer with simple beam and background correction. The samples were previously dissolved in hydrofluoric acid and diluted to the interval of measurement. The Cu loading on the catalyst was 6.0 wt.%.

The temperature-programmed desorption of NO or C_3H_6 was carried out using a Micromeritics TPD/TPR 2900 analyzer. The samples were housed in a quartz tubular reactor and pretreated in flowing helium (≥99.9990% purity), while heating at 15 °C min^{-1} up to the calcination temperature of the sample. After a period of 30 min at this temperature, the samples were cooled to 50 °C and saturated for about 30 min in a 4% NO/He or 4% C_3H_6/He stream. The catalyst was then allowed to equilibrate in a helium flow at 50 °C for 1 h. Next, the NO or C_3H_6 was desorbed by using a linear heating rate of 15 °C min^{-1} up to 300 °C. Temperature and detector signals were simultaneously recorded.

2.3. Catalyst activity measurements (NO SCR test)

Catalytic tests were carried out in a fixed-bed flow reactor working at atmospheric pressure. A temperature programmer was used with a K-type thermocouple installed in contact with the catalyst bed. The catalyst was equilibrated at each reaction temperature for 30 min before the analysis was started. The products were analyzed by a FTIR analyzer (Perkin-Elmer Spectrum GX) capable of measuring continuously and simultaneously the following species: NO, NO_2, N_2O, CO_2 and C_3H_6.

2.4. In situ FTIR measurements

In situ IR spectra were collected with a FTIR Perkin-Elmer Spectrum GX spectrometer, by accumulating 100 scans at a resolution of 4 cm^{-1}. The focused wavenumber range was 4000–1000 cm^{-1}. The sample was placed in the center of a high temperature reaction chamber with KBr windows (HARRICK). The temperature was measured with a K-type thermocouple and controlled with an automatic temperature controller (HARRICK).

Prior to each experiment, 0.05 g of catalyst was heated at a rate of 10 °C min^{-1} from room temperature to 400 °C. After a period of 30 min at this temperature, the sample was later cooled down to 200 °C at 10 °C min^{-1} in a He flow of 60 ml min^{-1}. After pretreatment, the background spectrum of a He flow of 25 ml min^{-1} was collected at 200 °C. Then, a flow of a gas mixture was switched to the reaction chamber at a flow rate of 25 ml min^{-1}, GHSV = 15,000 h^{-1}.

3. Results and discussion

Fig. 1 shows the IR spectra of Ti-PILC and Cu-Ti-PILC at 200 °C after pre-treatment previously described. Cu-Ti-PILC spectrum will be the background spectrum in all in situ IR runs carried out in this study. A broad band at 3700–3620 cm^{-1} is observed in both spectra, which is usually assigned to the oxygen–hydrogen stretching [26,28,35]. The intensity of this band is higher for Cu-Ti-PILC than for Ti-PILC; this fact can be attributed to the presence of Cu^{2+} ions over the Cu-Ti-PILC sample [22],

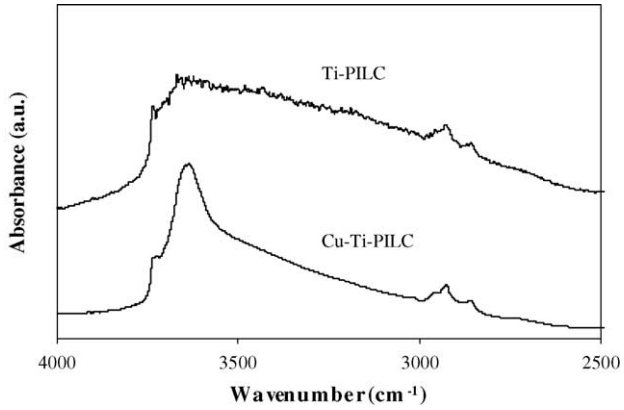

Fig. 1. IR spectra of Ti-PILC and Cu-Ti-PILC at 200 °C.

which can be like terminal and bridged Cu^{2+}–OH groups [28].

Fig. 2 shows the catalytic performance of Cu-Ti-PILC for the NO–SCR reaction. It is important to highlight that the most effective temperature, defined as the temperature of the maximum NO conversion to N_2, was around 235 °C. At this temperature the conversion was 55%. At higher temperatures, the NO conversion to N_2 decreases. According to Yang et al. [14] this decrease was due to the combustion of propene. For this reason, all in situ IR runs were carried out at 235 °C.

Fig. 3 shows IR spectra of the adsorbed species on Cu-Ti-PILC at 235 °C in flowing NO–O_2 as a function of the time of exposure. Strong bands can be observed at 1602, 1579, 1540, 1268 cm^{-1} and weak bands at 3700, 2971, 2887, 2586, 2191, 1753, and 1368 cm^{-1}. The band at 1368 cm^{-1} disappears at longer times. The intensity of the other bands increases with increasing times until the saturation of the catalyst after 120 min of exposure.

An increase in the intensity of the negative band at 3700 cm^{-1} after the admission of NO–O_2, which is due to ν(OH)-stretching of the H-bonded OH groups [28], suggests

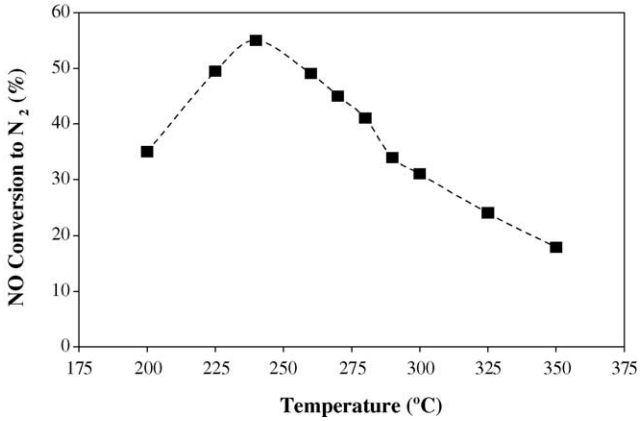

Fig. 2. NO conversion to N_2. Catalyst: Cu-Ti-PILC. Operation conditions: [C_3H_6] = 1000 ppm, [O_2] = 5%, [He] = balance. Flow rate = 125 ml min^{-1}, GHSV = 15,000 h^{-1}.

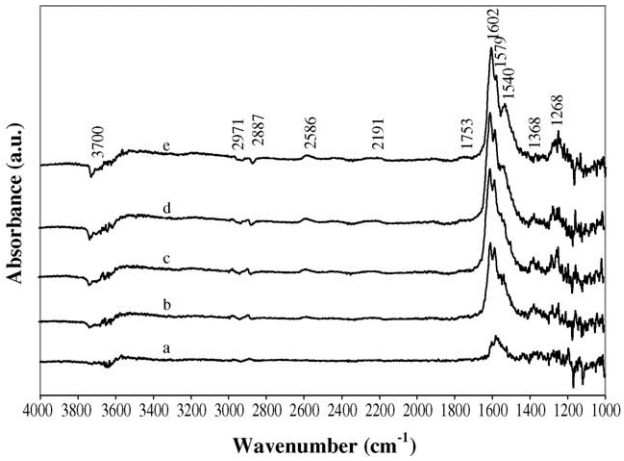

Fig. 3. IR spectra of adsorbed species over Cu-Ti-PILC in flowing NO–O_2 at 235 °C for (a) 2.5 min, (b) 15 min, (c) 30 min, (d) 60 min and (e) 120 min.

that terminal and bridged Cu^{2+}–OH groups are either affected by the nearby NO_x species or involved in the formation of the nitrate species as proposed for copper [28] and titania [36].

The region between 1625 and 1200 cm^{-1} is usually associated with NO_3^- species coordinated to the titania surface [37]. All the adsorption bands observed can be attributed to bridged nitrates at 1602 cm^{-1} (ν(N=O)) [28], monodentate nitrate at 1579 and 1540 cm^{-1} ($\nu_{as}(NO_2)$) and at 1268 cm^{-1} ($\nu_s(NO_2)$) [36].

Bands at 2900–2700 cm^{-1} may be originated by bridged nitrate (ν(N=O) + $\nu_{as}(NO_2)$) [38], while the band at 2586 cm^{-1} may be the consequence of bidentate nitrate (ν(N=O) + $\nu_s(NO_2)$). The band observed at 2191 cm^{-1} is attributed to N_2O [28]. The band at 1753 cm^{-1} can be related to $Cu^{2+}(NO)_2$ with vibration modes (ν_s(NO), (ν_{as}NO)) [26,38,39].

The spectrum in Fig. 4(a) was measured after pretreatment in flowing NO–O_2 for 120 min followed by a He purge for 20 min. The change in the flowing gas to C_3H_6–O_2

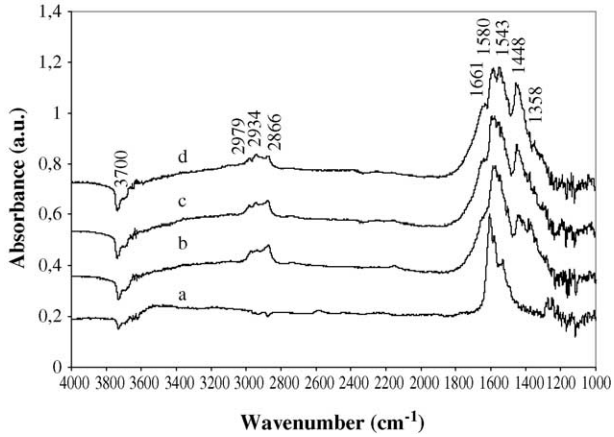

Fig. 4. IR spectra of adsorbed species over Cu-Ti-PILC at 235 °C. The catalyst was treated in flowing NO–O_2 for 120 min. The spectra were measured (a) after He purge for 20 min, followed by switching to flowing C_3H_6–O_2 for (b) 30 min, (c) 120 min and (d) 240 min.

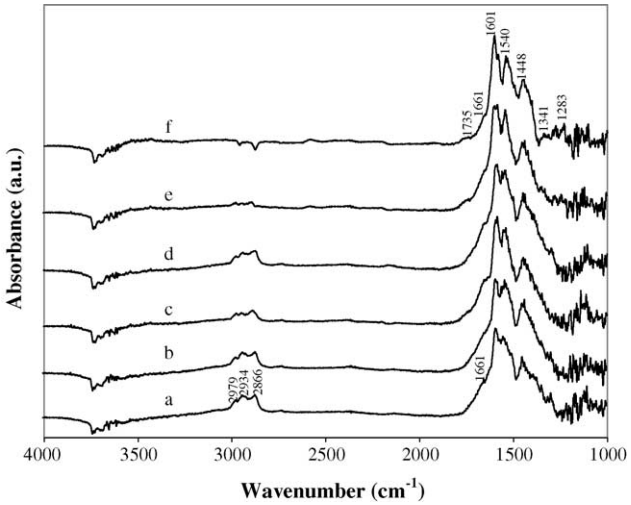

Fig. 5. IR spectra of adsorbed species over Cu-Ti-PILC at 235 °C. The catalyst was treated in flowing C_3H_6 (a) for 60 min. The spectra were measured (b) after He purge for 20 min, followed by switching to flowing NO-O_2 for (c) 10 min, (d) 30 min, (e) 60 min and (f) 120 min.

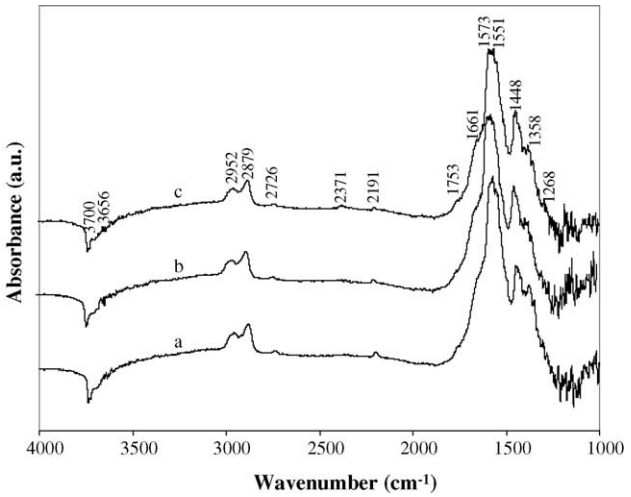

Fig. 6. IR spectra of adsorbed species over Cu-Ti-PILC at 235 °C (a) in flowing NO–O_2–C_3H_6–He for 120 min, followed by He purge for (b) 20 min (c) 40 min.

gave the other spectra (b–d), which are dependent on the time of exposure (from 30 to 240 min).

A negative band at 3700 cm^{-1} that increased with time appeared and bands at 2979, 2934 and 2866 cm^{-1} that gradually grow until the catalyst saturates after 240 min were also observed. The band at 3700 cm^{-1} corresponds to the OH stretching. Bands at around 2979, 2934 and 2866 cm^{-1} can be assigned to C–H asymmetric stretching [26,28,36,40,41].

The bands in the region 1650–1300 cm^{-1} increased with a longer time of exposure to the C_3H_6–O_2 stream. Chi and Chuang [26] assigned the bands at 1580 and at 1358 cm^{-1} to an organic nitro compound (C_3H_7–NO_2), and the band at 1661 cm^{-1} to an organic nitrito compound (C_3H_7–ONO). The band at 1448 cm^{-1} was assigned to acetate [39].

Fig. 5 shows IR spectra of adsorbed species over Cu-Ti-PILC at 235 °C. The catalyst was treated in flowing C_3H_6 (a) for 60 min. The spectra were registered after He purge for 20 min (b), followed by switching to flowing NO–O_2 for (c) 10 min, (d) 30 min, (e) 60 min, (f) 120 min. Spectrum (a) shows bands at 3000–2800 cm^{-1} that were assigned to C–H stret 0–1200 cm^{-1} that were assigned to both C=C stretching and C–H bending [26].

Bands at 3000–2800 cm^{-1} decreased after the flowing gas was switched to NO–O_2. The assignment of bands at 1650–1200 cm^{-1} in spectrum (f) was carried out as follows: 1601 cm^{-1} to NO_3^- bridged, 1579 and 1540 cm^{-1} to bidentate NO_3^-, 1448 cm^{-1} to monodentate NO_3^- [26,36], 1337 and 1283 cm^{-1} to bridging bidentate nitrate $(NO_3^-)_2$ [33].

Like in Fig. 3, the band at 1735 cm^{-1} grows with time of exposure to the NO–O_2 stream. This band is also related to $Cu^{2+}(NO)_2$ with vibration modes (ν_s(NO), ν_{as}(NO)) [26,38].

Besides, a shoulder, which was attributed by Chi and Chuang to an organic nitrito compound (C_3H_7–ONO) [26], is observed at 1661 cm^{-1}. This band is also observed in Fig. 4.

Fig. 6 shows the in situ IR spectra of adsorbates produced from flow of NO–O_2–C_3H_6–He over Cu-Ti-PILC at 235 °C for 120 min. While He purging, two different measurements were taken at 20 and 40 min intervals. Table 1 shows the assignment of bands.

The broad bands observed in Fig. 6 result from the overlapping of multiple bands. Although most of these bands cannot be unambiguously assigned, the bands in the regions of 1600–1200 and 2900–2700 cm^{-1} observed in Figs. 3–5 can be attributed to different nitrate species or to the different vibrations modes of C=C and C–H stretching.

In order to correctly assign the bands observed in Fig. 6 and understand the SCR reaction pathway, a study of the effect of NO concentration on the NO reduction and C_3H_6 combustion at different reaction temperatures over the Cu-Ti-PILC sam-

Table 1
Assignment of the infrared bands over Cu-Ti-PILC treated in flowing NO–O_2–C_3H_6–He for 120 min at 235 °C

Wavenumber (cm^{-1})	Assignment	References
3700	–OH stretching	[28]
3656	–OH stretching	[26,28,35]
2952	C–H asymmetric stretching bridged nitrate	[26,28,36,40,41]
2879	C–H asymmetric stretching bridged nitrate	[26,28,36,40,41]
2726	>C=O	[40,42,43]
2371	CO_2 gas	[26]
2191	N_2O	[28]
1735	$Cu^{2+}(NO)_2$	[38]
1661	organic nitrito compound (C_3H_7–ONO)	[26]
1573	Bidentate nitrate	[36]
1551	Bidentate nitrate	[36]
1448	CH_3COO^-	[26,36,39]
1358	Organic nitro compound C_3H_7–NO_2	[26]
1268	Bidentate nitrate	[39]

Measurements were taken while He purging for 20 and 40 min.

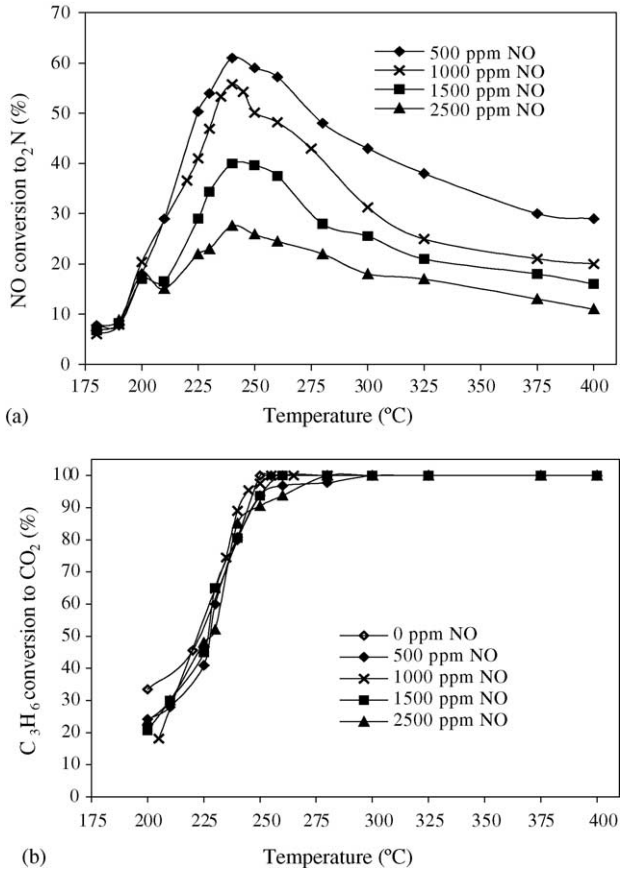

Fig. 7. Influence of the NO concentration on (a) NO conversion to N_2 and (b) C_3H_6 conversion to CO_2 at different reaction temperatures. Catalyst: Cu-Ti-PILC. Operation conditions: $[C_3H_6] = 1000$ ppm, $[O_2] = 5\%$, [He] = balance. Flow rate = 125 ml min^{-1}, GHSV = 15,000 h^{-1}.

ple was carried out. According to Fig. 7(a), it can be deduced that higher NO concentrations in the feed have a negative effect on the NO reduction to N_2. However, when NO concentration is increased, the C_3H_6 oxidation to CO_2 is not affected since, as shown in Fig. 7(b), all the curves are identical.

It could be possible to assume that NO and C_3H_6 have different affinity over the catalyst active sites. According to this, C_3H_6 adsorption over them would be higher and stronger than NO one. Thereby, C_3H_6 would react in the active sites producing hydrocarbon intermediates, which would be responsible for the NO reduction. An increase in NO concentration would not affect the number of C_3H_6 species adsorbed on the active sites, as they could not be displaced by NO. Thus, the proportion of NO species not converted would increase, so the NO conversion would decrease.

To verify this hypothesis, NO and C_3H_6 TPD experiments were carried out (Fig. 8). It can be observed that both the desorbed amount and the temperature to which the maximum desorption is obtained were clearly higher for C_3H_6 than for NO, confirming that the former has a stronger affinity to the catalyst active sites than the latter.

According to Chi and Chuang [26], these results could explain the appearance in the NO–O_2 coadsorption on Cu-Ti-PILC of the species $Cu^{2+}(NO_3^-)_2$ (Fig. 4). When the flowing gas is C_3H_6–O_2, C_3H_6 would remove the adsorbed $(NO_3^-)_2$ from Cu^{2+} species, and lead to reduction in Cu^{2+} to Cu^0/Cu^+. It is clear that C_3H_6 competes with NO–O_2 for the active sites of the catalyst, keeping Cu in either Cu^0 or Cu^+ state. This induces the formation of C_3H_7–NO_2 and acetate as potential intermediates, allowing that $(NO_3^-)_2$ turns into N_2 [18,26,31,44–48].

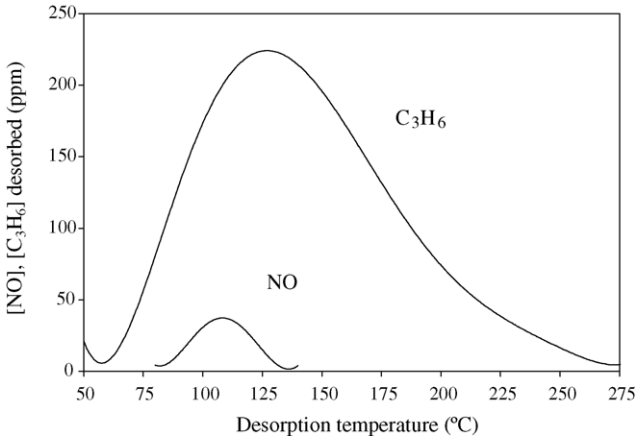

Fig. 8. NO and C_3H_6-TPD profiles obtained for the Cu-Ti-PILC.

On the other hand, the presence of the negative band at 3700 cm^{-1} (shown in Figs. 3 and 6), which is attributed to O–H stretching, is an evidence that the nitro group reacts with the hydroxyl group, thus forming nitrate [37,38]. This step was the one in the mechanism proposed by Sirilumpen et al. [28]. In this research, a small amount of N_2O was detected (Figs. 3 and 6). The presence of N_2O might be generated from the decomposition of the nitrate species: this process may take place on the Cu^+/Cu^0 sites [26,28,46,49].

The presence of Cu^{2+} ions and CuO aggregates on Cu-Ti-PILC [22,49] and the presence of a broad band in the region 3700–2900 cm^{-1}, due to the occurrence of free OH hydroxyl groups on the surface of this catalyst (Fig. 1), would justify the presence of the reaction intermediates proposed for Cu-Ti-PILC catalysts.

4. Conclusions

Adsorbed species on Ti–Cu–PILC in flowing NO–O_2 were tested using in situ FTIR spectroscopy. The NO–O_2 coadsorption produced different nitrates species, formed due to the presence of terminal and bridged Cu^{2+}–OH groups. These nitrates evolved into N_2 and a small amount of N_2O once the NO catalytic cycle was finished.

The experiment, where the catalyst was firstly pretreated in flowing NO–O_2, and then later treated in flowing C_3H_6–O_2, suggests the formation of the following reaction intermediates: C_3H_7–NO_2, acetate and different NO_3^- species. These reaction intermediates appeared when propylene and NO, in excess of oxygen, interacted with the active

sites of the catalyst. C_3H_6 not only removed the adsorbed NO_3^- from the Cu^{2+} species, but also led to the reduction of Cu^{2+} to Cu^0/Cu^{2+}, allowing CO_2 and N_2 formation.

In situ IR study of SCR of NO by propene showed that reaction intermediates were mainly NO_3^- species, C_3H_7–NO_2 and acetate. Cu^{2+}–OH groups reacted with the nitro group, thus forming nitrate. The decomposition of nitrate species generated N_2 and a small amount of N_2O. The adsorption of C_3H_6 on the catalyst active sites was higher and stronger than that of NO and allowed the formation of hydrocarbon intermediates (C_3H_7–NO_2 and acetate), which were responsible for the NO reduction.

Acknowledgment

Financial support by the Ministerio de Ciencia y Tecnología (CICYT) of Spain (Project PPQ2001-1195-C02-01) is gratefully acknowledged.

References

[1] C.N. Costa, T. Anastasiadou, A.M. Efstathiou, J. Catal. 194 (2000) 250.
[2] M. Shelef, Chem. Rev. 95 (1995) 209.
[3] M. Iwamoto, Catal. Today 29 (1996) 29.
[4] A.W. Aylor, S.C. Larsen, J.A. Reimer, A.T. Bell, J. Catal. 157 (1995) 592.
[5] Y. Li, J.N. Armor, Appl. Catal. B 5 (1995) 257.
[6] B.J. Adelman, T. Beutel, G.-D. Lei, W.M.H. Sachtler, J. Catal. 158 (1996) 327.
[7] K.A. Bethke, H.H. Kung, J. Catal. 172 (1997) 93.
[8] R. Burch, A.A. Shestov, J.A. Sullivan, J. Catal. 182 (1999) 497.
[9] Y.-H. Chin, A. Pisanu, L. Serventi, W.E. Alvarez, D.E. Resasco, Catal. Today 54 (1999) 419.
[10] D.K. Captain, M.D. Amiridis, J. Catal. 184 (1999) 377.
[11] S. Xie, M.P. Rosynek, J.H. Lunsford, J. Catal. 188 (1999) 24.
[12] F.C. Meunier, J.P. Breen, V. Zuzaniuk, M. Olsson, J.R.H. Ross, J. Catal. 187 (1999) 493.
[13] K. Shimizu, F. Okada, Y. Nakamura, A. Satsuma, T. Hattori, J. Catal. 195 (2000) 151.
[14] R.T. Yang, N. Tharappiwattananon, R.Q. Long, Appl. Catal. B 19 (1998) 289.
[15] M. Iwamoto, H. Furukawa, Y. Mine, F. Uemura, S. Mikuriya, S. Kagawa, J. Chem. Soc., Chem. Commun. 16 (1986) 1272.
[16] M.D. Amiridis, T. Zhang, R.J. Farrauto, Appl. Catal. B 10 (1996) 203.
[17] M. Shelef, Catal. Lett. 15 (1992) 305.
[18] C. Yokoyama, M. Misono, J. Catal. 150 (1994) 9.
[19] K. Shimizu, H. Kawabata, H. Maeshima, A. Satsuma, T. Hattori, J. Phys. Chem. B 104 (2000) 2885.
[20] K. Shimizu, H. Maeshima, H. Yoshida, A. Satsuma, T. Hattori, Phys. Chem. Chem. Phys. 2 (2000) 2435.
[21] R.T. Yang, W. Li, J. Catal. 155 (1995) 414.
[22] J.L. Valverde, A. De Lucas, P. Sanchez, F. Dorado, A. Romero, Appl. Catal. B 43 (2003) 43.
[23] J.L. Valverde, A. de Lucas, P. Sanchez, F. Dorado, A. Romero, Stud. Surf. Sci. Catal. 142A (2002) 723.
[24] J.L. Valverde, A. De Lucas, F. Dorado, R. Sun-Kou, P. Sanchez, I. Asencio, A. Garrido, A. Romero, Ind. Eng. Chem. Res. 42 (2003) 2783.
[25] J.L. Valverde, F. Dorado, P. Sanchez, I. Asencio, A. Romero, Ind. Eng. Chem. Res. 42 (2003) 3871.
[26] Y. Chi, S.S.C. Chuang, J. Catal. 190 (2000) 75.
[27] R. Burch, P.J. Millington, A.P. Walker, Appl. Catal. B 4 (1994) 65.
[28] M. Sirilumpen, R.T. Yang, N. Tharapiwattananon, J. Mol. Catal. A 137 (1999) 273.
[29] F. Poignant, J.L. Freysz, M. Daturi, J. Saussey, Catal. Today 70 (2001) 197.
[30] N. Bion, J. Saussey, M. Haneda, M. Daturi, J. Catal. 217 (2003) 47.
[31] A. Satsuma, T. Enjoji, K. Shimizu, K. Sato, H. Yoshida, T. Hattori, J. Chem. Soc., Faraday Trans. 94 (1998) 301.
[32] M. Shimokawabe, K. Tadokoro, S. Sasaki, N. Takezawa, Appl. Catal. A 166 (1998) 215.
[33] A. Shichi, A. Satsuma, T. Hattori, Appl. Catal. B 30 (2001) 25.
[34] S.-C. Shen, S. Kawi, J. Catal. 213 (2003) 241.
[35] A. Zecchina, S. Bordiga, G. Spoto, D. Scarano, G. Petrini, G. Leofanti, M. Padovan, C.O. Arean, J. Chem. Soc., Faraday Trans. 88 (1992) 2959.
[36] M. Kantcheva, J. Catal. 204 (2001) 479.
[37] K. Hadjiivanov, V. Bushev, M. Kantcheva, D. Klissurski, Langmuir 10 (1994) 464.
[38] M. Kantcheva, A.S. Vakkasoglu, J. Catal. 223 (2004) 352.
[39] J. Shibata, K. Shimizu, A. Satsuma, T. Hattori, Appl. Catal. B 37 (2002) 197.
[40] A.A. Davydov, Infrared Spectroscopy of Adsorbed Species on the Surface of Transition Metal Oxides, John Wiley & Sons, New York, 1990, p. 258.
[41] C.J. Pouchert, The Aldrich Library of Infrared Spectra, second ed., Aldrich Chemical Company Inc., Milwaukee, WI, 1975, p. 358.
[42] E. Finocchio, G. Busca, V. Lorenzelli, V.S. Escribano, J. Chem. Soc., Faraday Trans. 92 (1996) 1587.
[43] G.R. Bamwenda, A. Ogata, A. Obuchi, J. Oi, K. Mizuno, J. Skrzypek, Appl. Catal. B 6 (1995) 311.
[44] T. Tanaka, T. Okuhara, M. Misono, Appl. Catal. B 4 (1994) L1–L9.
[45] N.W. Hayes, R.W. Joyner, E.S. Shpiro, Appl. Catal. B 8 (1996) 343.
[46] K. Shimizu, H. Kawabata, A. Satsuma, T. Hattori, J. Phys. Chem. B 103 (1999) 5240.
[47] B. Djonev, B. Tsyntsarski, D. Klissurski, K. Hadjiivanov, J. Chem. Soc., Faraday Trans. 93 (1997) 4055.
[48] T. Okuhara, Y. Hasada, M. Misono, Catal. Today 35 (1997) 83.
[49] J.L. Valverde, F. Dorado, P. Sanchez, I. Asencio, A. Romero, Interfacial Applications of Environmental Engineering, Marcel Dekker Inc., New York, 2003, p. 39.